Sule Lamido University Journal of Science and Technology (SLUJST) Vol. 2 No. 1 [January, 2021], pp. 53-64

Mutual Coupling Reduction For Triple Band MIMO Antenna Using Stub Loading Technique

Adamu Halilu Jabire[1*], Aminu Gambo Abdullahi[2], Sani Saminu[3], Adamu Mohammed Jajere[4]
Abubakar Muhammad Sadiq[5]

1. *Dept. of Electrical and Electronics Engineering, Taraba State University, Jalingo, Nigeria,*
2. *National Commission for Museums and Monument, Kano, Nigeria,* a.aminu51@yahoo.com
3. *Dept. of Biomedical Engineering, University of Ilorin, Ilorin, Nigeria,* saminu.s@unilorin.edu.ng
4. *School of Microelectronics, Tianjin University, Tianjin, P.R. China, mainajajere@tju.edu.cn*
5. *School of Microelectronics, Tianjin University, Tianjin, P.R. China, amsadiq32@tju.edu.cn*

*Corresponding author: adamu.jabire@tsuniversity.edu.ng.

Abstract

This paper presents a mutual coupling reduction using stub and partial ground structure. The driven analysis comprises four antennas that are placed orthogonal to each other. A decoupling network is proposed, which consists of one long stub extended between the four defected ground structure for electromagnetic interaction reduction. The proposed antenna has triple-band frequencies at 3 GHz, 5.5 GHz, and 7.1 GHz. The performance of the four by four antenna arrays is evaluated based on envelope correlation coefficient, isolation, mean effective gain, channel capacity loss, total active reflection coefficient, and diversity gain. The results strongly support the applicability of fifth-generation sub 6 GHz applications.

Keywords: *Multiple Input Multiple Output Antenna, Mutual Coupling, Decoupling Structure, Isolation*

1. Introduction

One of the critical features of the fifth-generation (5G) microwave circuit is multiple-input-multiple-output (MIMO). MIMO techniques can be characterized when multiple antennas are used at both transmitting and receiving end. The main idea of the MIMO system is that sampled signals in the spatial terrain at both terminals are integrated to elevate the data rate, enhance the quality of the Communication and create precise multiple parallel spatial information. The year 2020 marks the commercial launch of 5G in China. The spectrum at which the 5G will operate is the millimeter-wave range, although there is a significant path loss in that frequency as compared to the sub 6GHz spectrum (Hassan et al., 2019). Why MIMO? It is all about the channel capacity of the system whereby the channel capacity depends on bandwidth and signal to noise ratio (Sanae et al., 2019). How do we increase the channel capacity of the system? To do that is either we increase the bandwidth of the system, which sometimes is not accessible due to resource limitations, or we can work on the signal to noise ratio; these two options are amendable to increase the channel capacity of the system (Min et al., 2019; Jabire, Abdu, et al., 2019; Jabire, Zheng et al., 2019). Utilizing multiple antennas at one end of the terminal was mainly for the diversity and estimation of directions of arrival, which leads to spatial MIMO/diversity and beamforming. Concentrating the energy to the desired direction increases the signal-to-noise ratio (SNR), which is called beamforming in the existence of random fading caused by multipath propagation. The signal to noise ratio will be enhanced by adding the output non-correlated antenna element, which is the main idea of space diversity.

2. Related Works

Antenna physical limit and electromagnetic interaction among the MIMO radiating elements are one of the challenges in the MIMO antenna system (Qian et al., 2018). When several radiating features are situated near each other, the fields generated by one antenna changes the current distribution on the neighboring elements. Therefore, the impedance matching and radiation pattern of each MIMO element are assigned based on the presence of other items (Dabas et al., 2018; Jeet et al., 2020; Mukesh, 2020). Many methods have been reported recently to reduce the mutual coupling of n x n MIMO antennas. The utilization of a metamaterial structure showed to be a successful strategy to minimize the mutual coupling between n x n MIMO antennas (Chandan et al., 2020; Dipesh et al., 2020). The effectiveness of defected ground structures has been exhaustively validated in

reducing electromagnetic suppression within different MIMO antennas (Vara et al., 2020; Chouhan et al., 2018; Vandana et al., 2018). Split rectangular loop resonator has been employed in (Jabire, Zheng, et al., 2019) to lower the electromagnetic interaction among the 2x2 MIMO antenna.

A letter presented in (Megha & Jayakumar, 2020; Kumar et al., 2020; Patchala et al., 2020), a complementary split-ring resonator (CSRR) has been studied in which, within the operation bands, a negative equivalent permeability is attained. An additional method called the neutralization line is utilized in decreasing the EMI between the MIMO antennas (Saleh et al., 2020; Luo et al., 2019). A multiport decoupling or matching network, including a negative permittivity, has been proposed to improve the inter-element isolation of a 4x4 antenna array (Cheng Yi-Feng & Cheng Kwok-Keung, 2020). This paper presents a simple and effective decoupling technique for decreasing the mutual coupling effect between the four MIMO antennas. A stub is placed symmetrically in between the ground plane of the MIMO antenna. The stub helps in absorbing the EMI between the antennas, which lead to the enhancement of inter-element isolation. The results demonstrate a reduced mutual coupling of less than 15dB at 3GHz, less than 30dB at 5.5GHz, and less than 15dB at 7.1GHz. Section II is the related works; Section III describes the evolution of the microwave circuit. Section IV show and discuss the simulated results of the 4x4 MIMO antenna. Section V is the MIMO system metrics. A conclusion is finally drawn in Section VI.

3. Design Evolution

Figure 1 below shows the geometry of the proposed four feed linearly polarized MIMO antenna to operate at three bands of frequencies. The antenna is composed of an L- shaped radiator printed on an FR4 substrate $(\varepsilon_r = 4.3, \tan\delta = 0.025)$. The distance between the four antennas was not too vast, which is why the decoupling structure was employed to decrease the electromagnetic interaction among the radiators. To further enhance the isolation, a stub is applied from the partial or defected ground structure by placing the stub to touch the end of the ground plane. The stub plays a significant role in reducing the mutual coupling effect. The antenna parameters are summarized in table 1. A finite size of 60mm x 10mm ground plane was used for every single MIMO all through the paper. The MIMO antenna involves a general scope of 60mm x 60mm x 1.6mm. The size of the stub is 50mm x 2mm; figure 2 is the $|S_{21}|$ of the proposed MIMO microwave circuit (antenna) before and after the introduction of the stub. It clearly shows that the isolation technique achieves a comparable enhancement with a simplified realization process. Each of the four-element is fed with a 50Ω microstrip feed line for perfect impedance matching. The connector used can support up to 30 GHz. All the design and simulation of this work are carried off in the commercial full-wave electromagnetic solver, computer simulation technology (CST) 2017.

4. Results and Discussion

The proposed MIMO antenna has been simulated to validate the performance. The S_{11} of the antenna with and without decoupling configuration unveils in figure 3. As clearly depicted, employing a decoupling form provides an additional useful frequency of 5.5GHz wireless local area network (WLAN). It is apparent that stub expands isolation as well as lessen the mutual coupling between the 4x4 MIMO system. The separation among the four antenna elements is depicted in Figure 4. The S_{21} is above 15dB at the frequency of interest. Simulated 2D far-field patterns for the MIMO antenna at 3GHz, 5.5GHz, and 7.1GHz in E and H planes are shown in figure 5. The pattern shape is Omni-directional. The viability of utilizing a stub as a decoupling structure is appeared by examining the current dispersion on the antenna's surface current at 3GHz, 5.5GHz, and 7.1GHz. It is given in figure 6 with excitation at port one while the remaining ports being terminated.

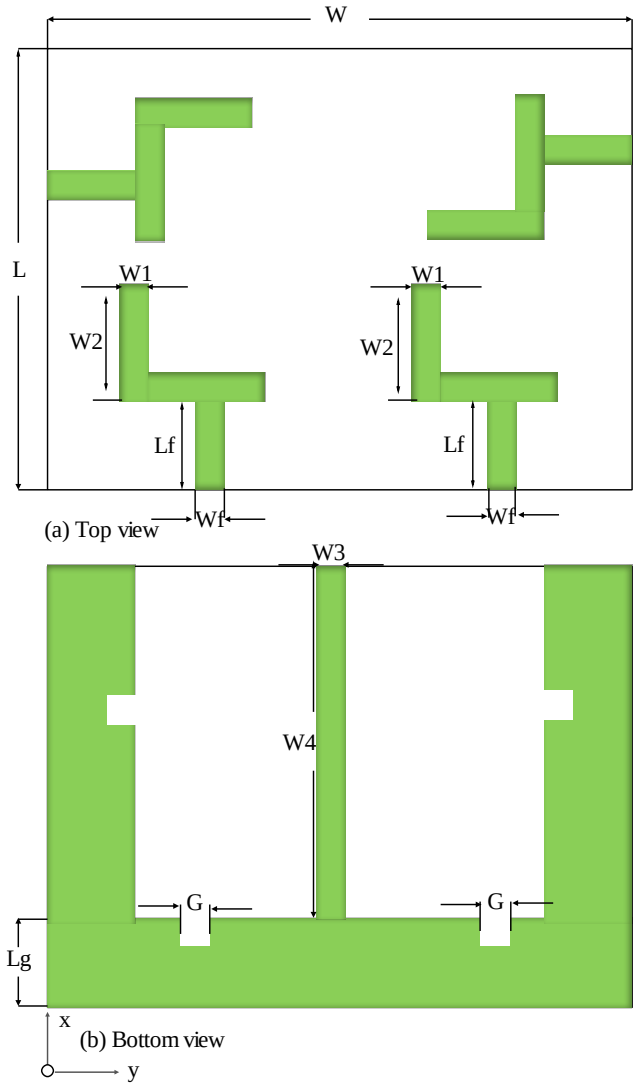

Figure 1. 4 x 4 MIMO Antenna Geometry

Table 1. Minimized 4 x 4 MIMO antenna parameters

Parameter	Size(mm)	Parameter	Size(mm)
G	4	W_1	3
L	30	W_2	10
L_F	11.05	W_3	2
L_G	10	W_4	50
W	30	W_F	3

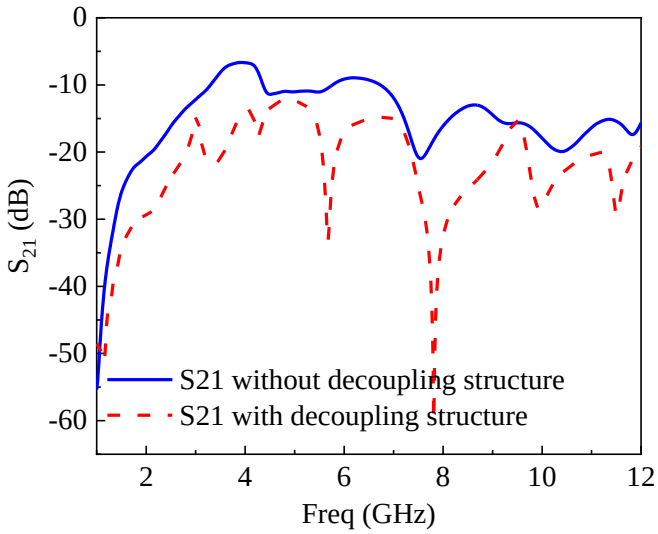

Figure 2. Parametric isolation of MIMO antenna

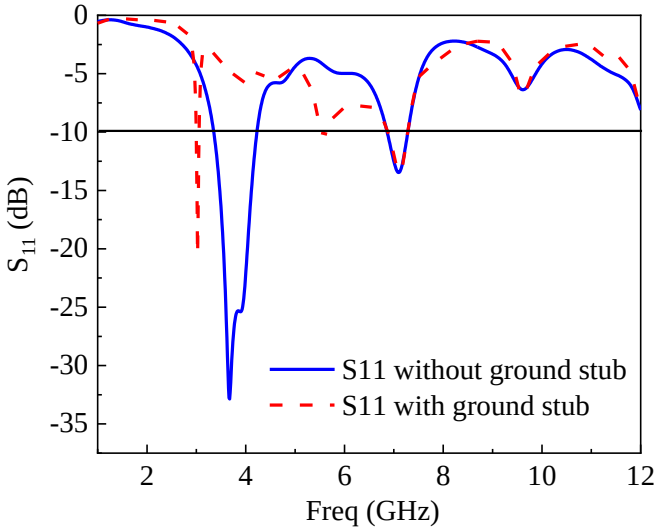

Figure 3. $|S_{11}|$ with and without decoupling structure

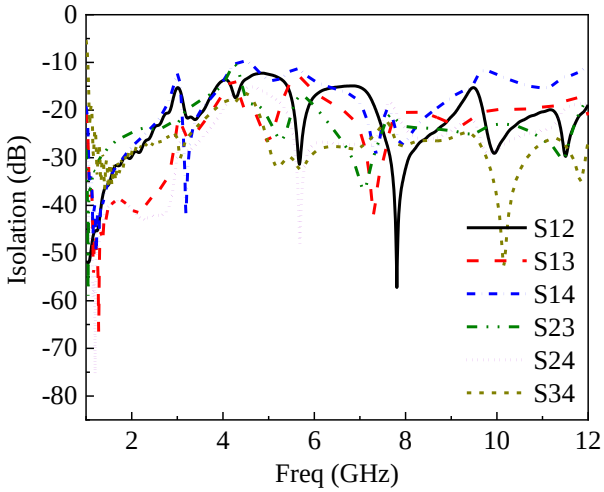

Figure 4. Isolation of the proposed 4 x 4 MIMO antenna

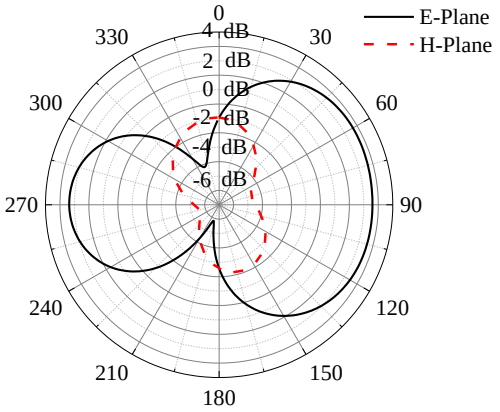

(a)

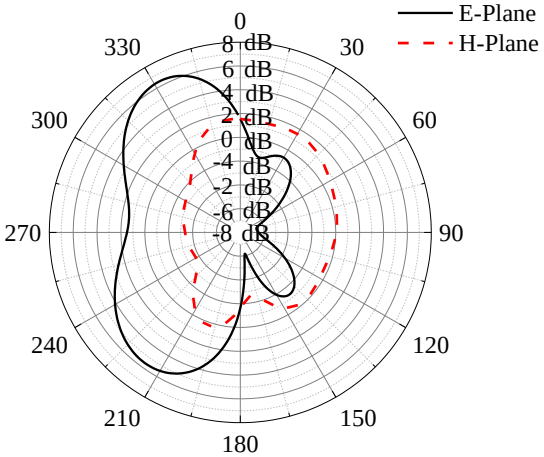

(b)

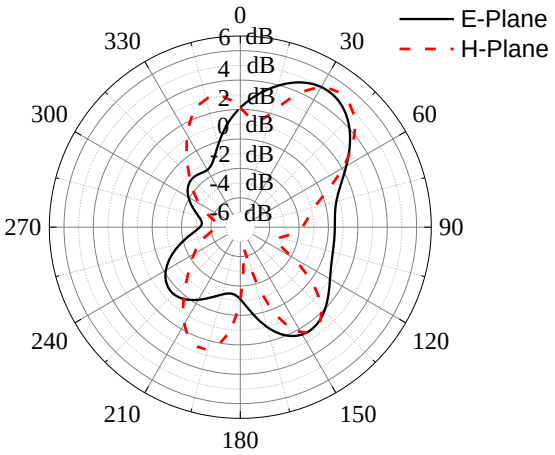

(c)

Figure 5. Radiation pattern of 4X4 MIMO antenna (a), 3GHz, (b) 5.5GHz, (c) 7.1GHz

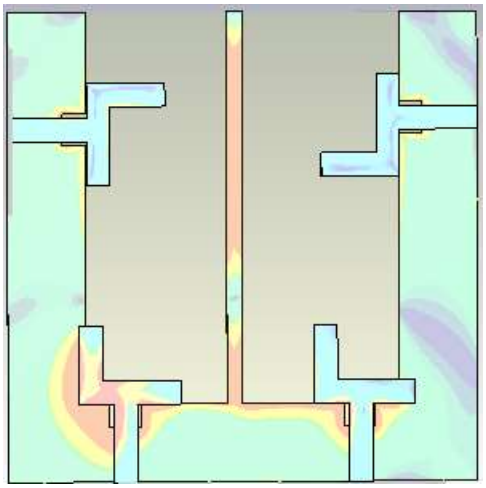

(a)

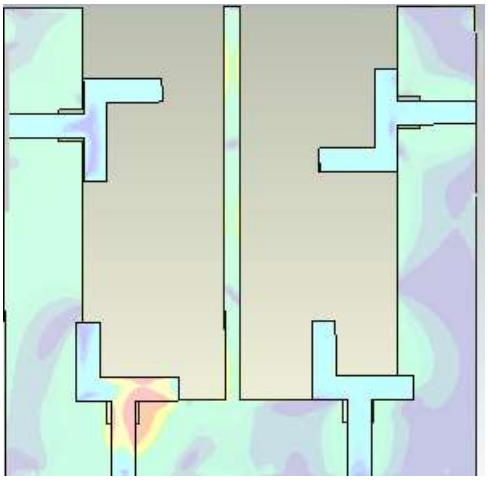

(b)

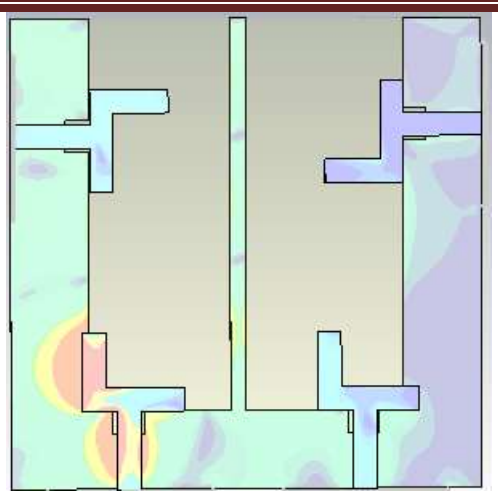

(c)

Figure 6. Surface current density: (a), 3GHz, (b) 5.5GHz, (c) 7.1GHz when port 1 is excited

5. MIMO Performance

A variable that serves as the determinant factor for the coupling coefficient between the MIMO antenna is called the envelope correlation coefficient (ECC). Virtually, the ECC factor must be lower than 0.5 (Elwi, 2018). For two or more antennas, The ECC (ρe) is computed from the far-field radiation pattern as in equation 1. The ECC plot is shown in Figure 7, which is lower than 0.01 over the band of interest.

$$\rho e = \frac{\left|\iint_{4\pi}\left[\vec{F}_1(\theta,\phi)\times\vec{F}_2(\theta,\phi)d\Omega\right]^2\right|}{\left|\iint_{4\pi}\left[\vec{F}_1(\theta,\phi)\right]^2 d\Omega\right|\left|\iint_{4\pi}\left[\vec{F}_2(\theta,\phi)\right]^2 d\Omega\right|} \tag{1}$$

Where S11, S12, S21, and S22 are the S-parameter of the MIMO antenna array. The diversity gain of the MIMO antenna is calculated using ECC as

$$DG = 10\sqrt{1-ECC^2} \tag{2}$$

The "diversity gain curve" is shown in figure 8. It is almost 10dB. The microwave circuit unveils good correlation and diversity performance. Another determinant factor that studies the coupling coefficient is the total active reflection coefficient (TARC), which is defined in terms of the incident and reflected power. TARC is calculated using equation 3, which is dependent on the S-parameter, say S_{11}, S_{12}, S_{21}, and S_{22}. The "TARC curve" is shown in figure 9.

$$TARC = \frac{\sqrt{\left|S_{11}+S_{12}e^{j\theta}\right|^2+\left|S_{22}+S_{21}e^{j\theta}\right|^2}}{\sqrt{2}} \tag{3}$$

Channel capacity must be taken into account to assess the execution of the MIMO antenna. Channel capacity loss depends on the number of antenna elements with a specific assumption (Muhammad et al., 2016.). The CCL illustrated in figure 10 is calculated using equation 4 to equation 7, which is plotted using Matlab 2018a. The plot depicts that the CCL is less than 0.01 at 5.5GHz and less than 0.5 at both 3GHz and 7.1GHz, respectively.

$$C_{loss} = -\log_2 \det(\alpha^R) \tag{4}$$

$$\text{Where } \alpha^R = \begin{bmatrix} \alpha_{11} & \alpha_{12} \\ \alpha_{21} & \alpha_{22} \end{bmatrix} \tag{5}$$

$$\alpha_{ii} = 1 - \left(\sum_{j=1}^{N} \left| S_{ij} \right|^2 \right) \tag{6}$$

$$\alpha_{ij} = -\left(S_{ii}^* S_{ij} + S_{ji}^* S_{ij} \right) \tag{7}$$

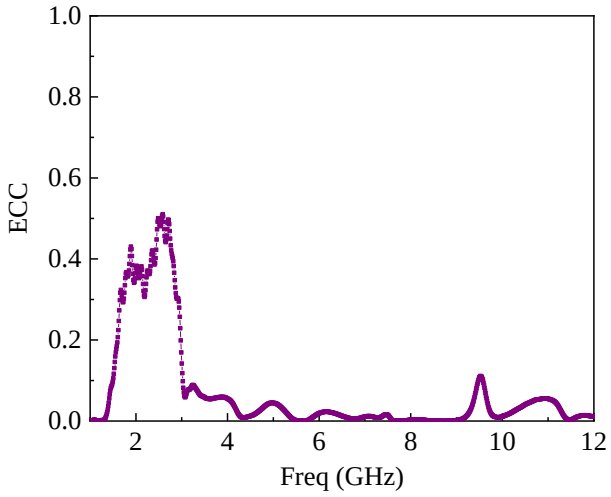

Figure 7. ECC of 4x4 MIMO antenna system

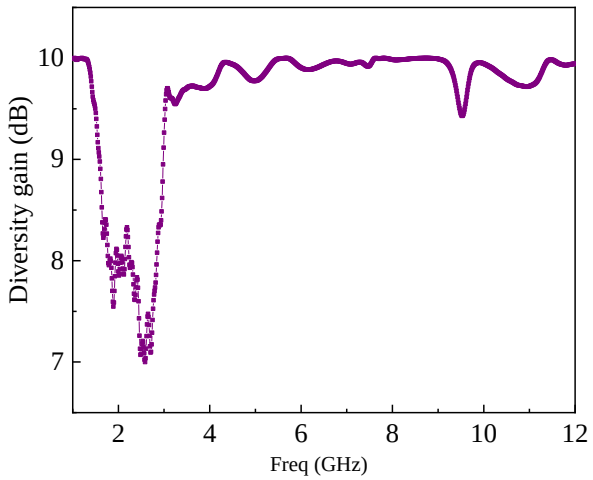

Figure 8. Diversity gain of 4x4 MIMO antenna system

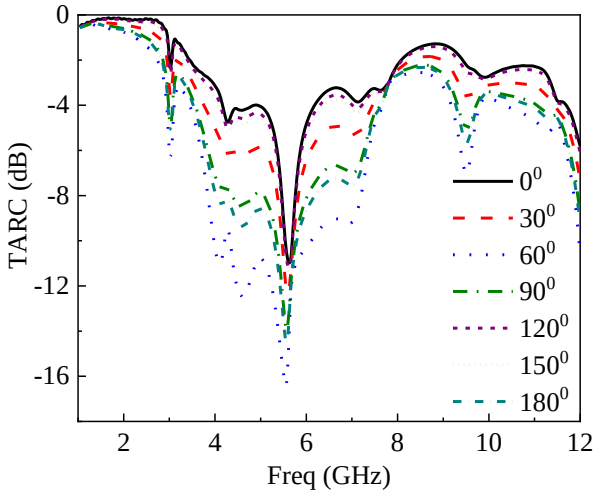

Figure 9. TARC of MIMO antenna system when θ changes from 0 to 180 degrees

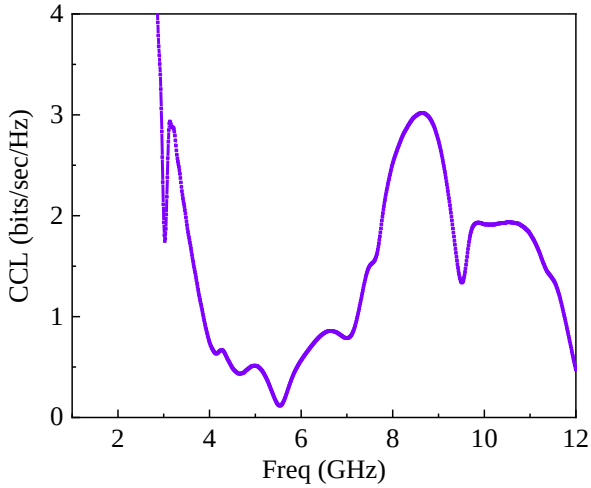

Figure 10. CCL of 4x4 MIMO antenna

The antenna mean effective gain (MEG) is defined as the ratio of the average power received at the microwave circuit (antenna) to the sum of the average power of the vertically and horizontally polarized waves received by an isotropic antenna (Khalil Al-Ani et al., 2020). Figure 11 shows the MEG, which is less than -3dB. It can be calculated as

$$MEG = 0.5\left[1 - \sum_{j=1}^{N} \left|S_{ij}\right|^2\right] \tag{8}$$

Where N is the number of antenna elements, the simulated realized gain is provided in figure 12. The comparison of the proposed 4X4 MIMO antenna with other reported antenna is classified in table 2; it is clear that the proposed antenna displays more bands and high isolation between elements.

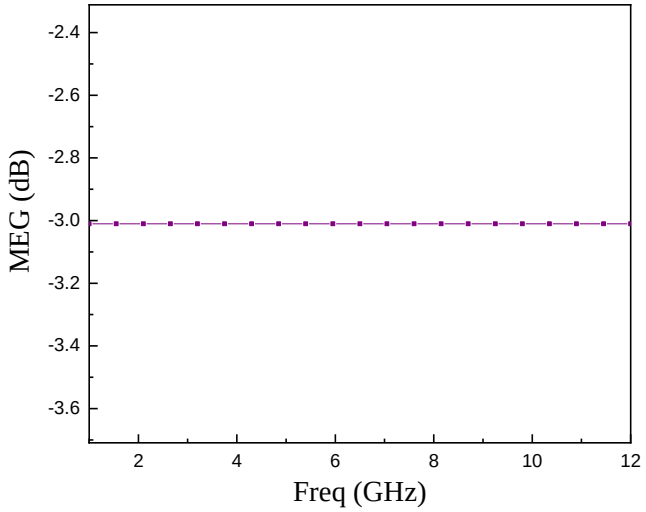

Figure 11. MEG of 4x4 MIMO antenna

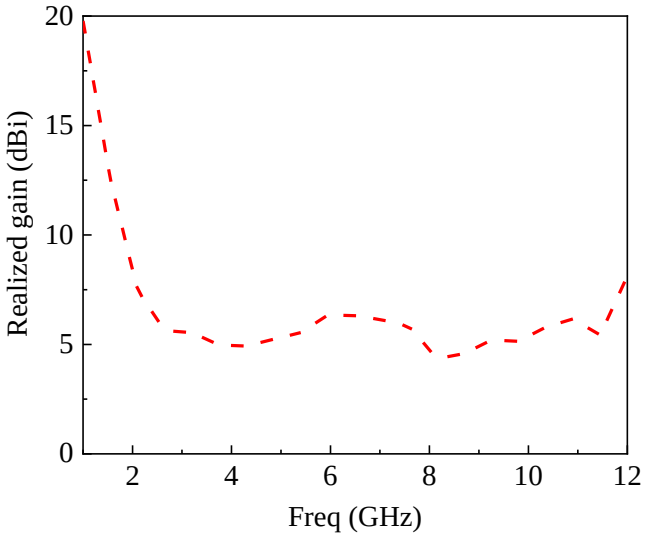

Figure 12. Realized gain of 4x4 MIMO antenna

Table 2. Comparison of the proposed 4x4 MIMO antenna with other planar MIMO antennas

Reference	Decoupling structure	Bands	Isolation
[1]	Mesh type resonator	Single	19.5
[5]	-	Single	22
[12]	-	Single	18
[19]	Split resonator	Triple	15
[24]	EBG	Single	48
This work	Stub	Triple	20

6. Conclusion

This paper presents a mutual coupling reduction with the help of stub employed in the ground plane. A 4x4 L-shaped MIMO Antenna is proposed, and several diversity metrics such as ECC of lower than 0.1, diversity gain of almost 10dB, TARC of lower than 0dB, mean effective gain of less than -3dB, and CCL of less than 0.35bits/sec/Hz were obtained. The obtained simulated results are perfect for 5G sub 6 GHz applications

Acknowledgment

This research is supported by the Department of Electrical and Electronics Engineering Taraba State University Jalingo for providing funds.

Reference

Chandan K. G., Manish P., Rahul K., & Saurabh P. (2020). Mutual Coupling Reduction of Microstrip MIMO Antenna using Microstrip Resonator. *Wireless Personal Communication,* 112, pp. 2047-2056.

Cheng Y. & Cheng K. M. (2020). Compact Wideband Decoupling and Matching Network Design for Dual-Antenna Array. *IEEE Antennas and Wireless Propagation Letters,* 19(5), pp. 791-795.

Chouhan S., Panda D. K., Gupta M., & Singha S. (2018). Multiport MIMO antennas with mutual coupling reduction techniques for modern wireless transceive operation: A review. *International J. RF Microw Computer-Aided Engineering,* 28: e21189.

Dabas T., Gangwar D., Kanaujia B. K., & Gautam A. K. (2018). Mutual Coupling Reduction Between Elements of UWB MIMO Antenna using Small Size Uniplanar EBG Exhibiting Multiple Stopbands. *International Journal of Electronics and Communication,* 93, pp. 32-38.

Dipesh K., Vivek S., Cher M. T., Vani P., & Nirdosh T. (2020). Optimization of a T-shaped MIMO Antenna for the Reduction of EMI. *Applied Science,* 10(0), pp. 1-15.

Elwi T. A. (2018). A miniaturized folded Antenna Array for MIMO Applications. *Wireless Personal Communication,* 98(2), pp. 1871-1883.

Hassan MN, Chu S, & Bashir S. (2019). A DGS Monopole Antenna Loaded with a U-shape Stub for UWB MIMO Applications. *Microwave Optical Technological Letters*, 61, pp. 2141-2149.

Jabire A. H., Abdu A., Samin S., Sadiq A. M., & Mohammed J. A. (2019). Isolation Frequency Switchable MIMO Antenna for PCS, WiMAX, and WLAN Application. *Elektrika Journal of Electrical Engineering,* 18(3), pp. 27-33.

Jabire A. H., Zheng H., & Abdu A. (2019). Split Rectangular Loop Resonator Inspired MIMO Monopoles for GSM/LTE/WLAN Applications, *Journal of Communications,* 14(6), pp. 511-517.

Jabire A. H., Zheng H., Abdu A., & Song Z. (2019). Characteristic Mode Analysis and Design of Wideband MIMO Antenna Consisting of Metamaterial Unit Cell, *Electronics,* 8(1), pp. 1-14.

Jeet B., Abhik, G., & Rowdra G. (2020). Design and Analysis of a Compact UWB MIMO Antenna Incorporating Fractal Inspired Isolation Improvement and Band Rejection Structure. *Inter. Journal of Electronics and Communications,* 122, pp. 1-9.

Khalil N. M., Shareef O. A., Mosleh M. F., & Abd-Alhameed R. A. (2020). A Design of MIMO Prototype in C-Band Frequency for Future Wireless Communications. *Advanced Electromagnetics,* 9(1), pp. 78-84.

Kumar A., Ansari A. Q., Kanaujia B. K., Kishor J., Kumar S. (2020). An Ultra-compact two-port UWB-MIMO Antenna with Dual Band-notched Characteristics. *Int. J. Electron. Commun. (AEÜ)* 114 152997, pp. 1-12.

Luo S., Li Y., Xia Y., & Zhang L. (2019). A Low Mutual Coupling Antenna Array with Gain Enhancement using Metamaterial Loading and Neutralization Line Structure. *ACES Journal*, 34(3), pp. 411-418.

Megha M. K., Jayakumar M. (2020). Design and Analysis of Circularly Polarized Dual Patch Antenna with Improved Isolation for MIMO Satellite. *International Journal of Microwave and Optical Technology*, 15(2), pp. 155-158.

Min L., Bing G. Z., & Cheung S. W. (2019). Isolation Enhancement for MIMO Patch Antennas Using Near-Field Resonators as Coupling-Mode Transducers. *IEEE Transactions on Antennas and Propagation*, 67(2), pp. 755-764.

Muhammad S. K., Antonio-Daniele C., Adnan I., Sajid A., & Benjamin D. B. (2016). A Compact Dual Polarized Ultra-Wideband Multiple-Input-Multiple-Output Antenna. *Microwave and Optical Technology Letters*, 58(1), pp. 163-166.

Mukesh K. K. (2020). Metamaterial Based Circularly Polarized Four-port MIMO Diversity Antenna Embedded with a Slow-wave Structure for Miniaturization and Suppression of Mutual Coupling, *Inter*. *Journal of Electronics and Communications,* 121, pp. 1-10.

Patchala, K., Rao Y. R., Prasad A. M. (2020). Triple Band-notch Compact MIMO Antenna with Defected Ground Structure and Split Ring Resonator for Wideband Applications. *Heliyon* 6 e03078, pp. 1-7.

Qian K., Huang G., Liang J., Qian B., & Yuan T. (2018). An LTCC Interference Cancellation Device for Closely Spaced Antenna decoupling, *IEEE Access* 6, pp. 68255-68262.

Saleh A. M., Nagim T. A., Abd-Alhameed R. A., Noras J. M. & See C. H. (2020). Mutual Coupling Reduction of Dual-band Uniplanar MIMO System using Neutralization Line Technique. *Applied Computational Electromagnetic Society Journal*, 35(2), pp. 176-186.

Sanae El., Abdelfatteh H., & Hayat, J. (2019). Road to 5G: Key enabling technologies. *Journal of Communication*, 14(11), pp. 1034-1048.

Vandana S. & Shikha N. (2018). Two Element Compact UWB Diversity Antenna with a Combination of DGS and Parasitic Elements, *Wireless Personal Communication*, 98, pp. 2901-2911.

Vara P. K. & Venkata P. M. (2020). A slot-shape EBG Structure for Improving the Isolation Between Patch Arrays. *International Journal of Microwave & Optical Technology*, 15(3), pp. 269-278.